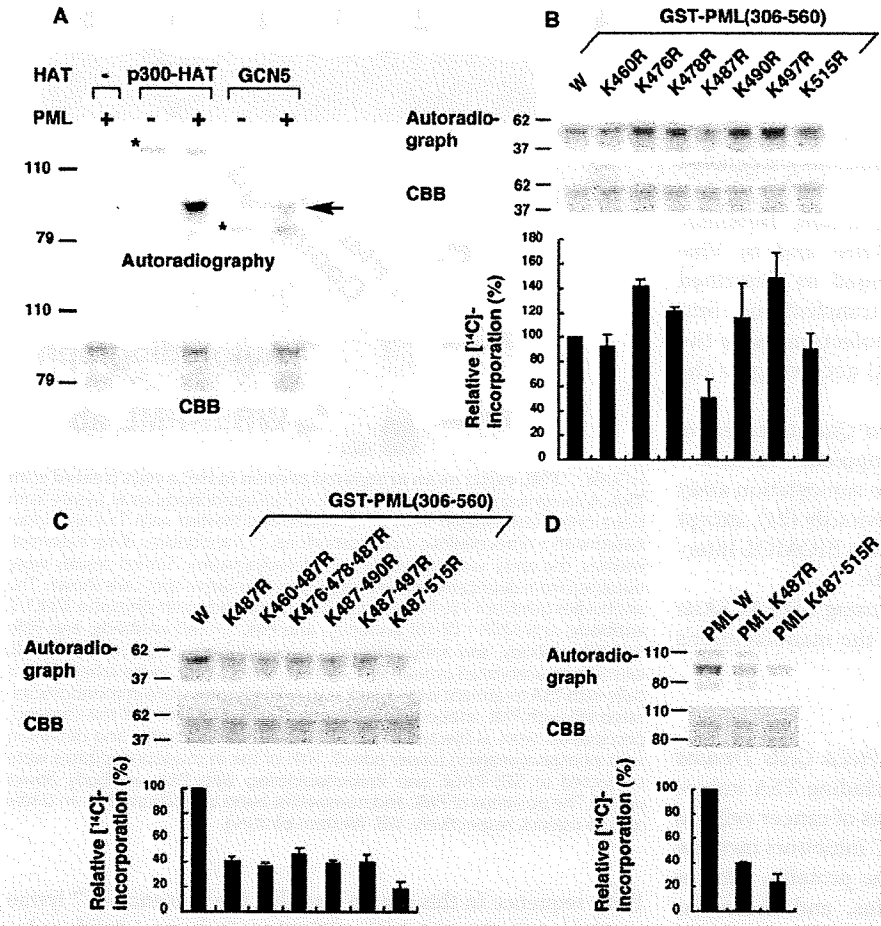

FIGURE 2. **PML acetylation *in vitro*.** *A*, PML is acetylated by p300 and GCN5. GST-PML was incubated with [^{14}C]acetyl-CoA and the indicated HATs. The reaction mixtures were subjected to SDS-PAGE, Coomassie Brilliant Blue (*CBB*) staining, and autoradiography. The positions of acetylated PML and acetylases are indicated by an *arrow* and *asterisks*, respectively. *B* and *C*, identification of PML acetylation sites. Wild-type or mutant GST-PML (amino acids 306–560) were subjected to *in vitro* acetylation by p300-HAT as in *A*. ^{14}C incorporation into each GST-PML construct was quantified using phosphorimaging. A representative phosphorimaging scan (*top panel*), the corresponding CBB-stained electrophoretogram (*middle panel*), and the quantitation of the ^{14}C incorporation for each mutant, relative to the wild-type PML construct (*bottom panel*), are presented. The averages of three independent analyses and standard deviations are shown. *D*, mutation of lysines in full-length PML reduced acetylation by p300. Wild-type or mutant GST-PML (full-length) were subjected to *in vitro* acetylation assays as described in *B*.

Next, we tested whether PML acetylation is induced by TSA. Similarly to the case of p300 coexpression, TSA treatment enhanced PML W acetylation, whereas acetylation of PML M was significantly reduced and showed no significant response to TSA treatment (Fig. 3*B*, *top panel*). Our results suggest that PML is an acetylation target of TSA and that PML acetylation in response to TSA largely occurs at the sites of acetylation by p300.

Acetylation of PML in Response to TSA Is Associated with Enhanced PML Sumoylation—Because one of the PML acetylation sites, lysine 487, is located in the putative nuclear localization signal (amino acids 476–490), we first examined whether PML acetylation affected its nuclear localization to see the effect of acetylation on PML function. However, TSA treatment and the acetylation-defective mutation did not obviously affect PML nuclear localization or accumulation to NBs in immunofluorescent staining (supplemental Fig. S3). We next investigated whether PML acetylation affected its sumoylation, which is required for PML to exercise many of its functions. We set up an *in vivo* sumoylation system in which conjugation of SUMO to PML could be detected by Western analysis, resulting in the appearance of a novel 100-kDa protein expected to be sumoylated PML (21). In this system, coexpression of p300 and exposure to TSA resulted in a significant increase in sumoylation of PML W, whereas sumoylation of PML M was weak and not obviously affected by these treatments (Fig. 4, *A* and *B*). These results suggest the possibility that PML acetylation at lysines 487 and 515 enhances its sumoylation. Next, to verify that acetylated PML is directly sumoylated, we set up an *in vitro* sumoylation system in which recombinant HA-tagged PML protein was incubated with recombinant SUMO E1 and E2 ligase and SUMO with or without a prior acetylation reaction using [^{14}C]acetyl-CoA. Autoradiography visualizing only acetylated PML demonstrated that acetylated PML was efficiently sumoylated (Fig. 4*C*, *upper panel*). Of note, sumoylation efficiency observed in the autoradiograph was much higher than that in immunoblotting with anti-HA antibody where acetylated and nonacetylated PML were visualized (Fig. 4*C*, *upper panel*, *lane 2 versus lower panel*, *lane 2*). These results indicate that acetylated PML may be preferentially sumoylated *in vitro*.

PML Acetylation May Play an Important Role in TSA-induced Apoptosis—TSA treatment induces apoptosis in HeLa cells by unknown mechanisms (16). In our previous study, PML sumoylation plays an important role in As_2O_3-induced apoptosis (21). Given our findings that PML acetylation is associated with increased PML sumoylation, this may represent one of the mechanisms of TSA-induced apoptosis. We first examined whether PML was involved in TSA-induced apoptosis. For this purpose, we established HeLa cells stably transfected with an expression vector for small hairpin RNA against PML and an empty control vector and designated them as PML KD HeLa and control KD HeLa, respectively. Successful knocking down of PML was confirmed by immunofluorescence analysis with an anti-PML antibody (supplemental Fig. S4). TSA treatment caused the appearance of a sub-G_1 peak in cell cycle analysis, a marker of apoptosis, in both cells. However, the ratio of apoptotic cells was reduced by ~60% in PML KD HeLa compared with control KD HeLa, suggesting the involvement of PML in

TSA-induced apoptosis (Fig. 5*A* and supplemental Fig. S5). We examined further using PML$^{-/-}$ MEFs. Notably, overexpression of PML W in PML$^{-/-}$ MEFs substantially increased TSA-induced apoptosis relative to cells transfected with an empty vector, whereas, PML M displayed an impaired ability to mediate apoptosis in response to TSA (Fig. 5*B* and supplemental Fig. S6). An equal expression level of PML between PML W and PML M transfectants was confirmed (supplemental Fig. S6). These results further support the involvement of PML in TSA-induced apoptosis and suggest the importance of PML acetylation in conferring apoptosis by TSA.

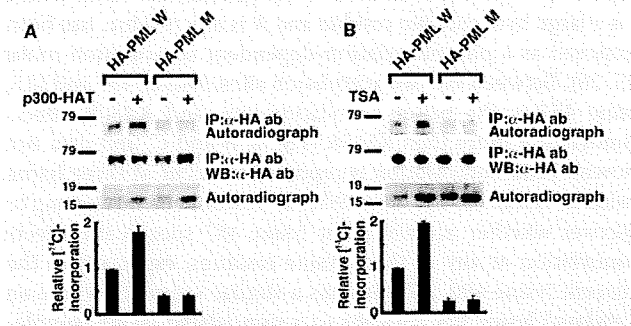

FIGURE 3. **PML acetylation *in vivo*.** *A*, PML acetylation is induced by p300 cotransfection *in vivo*. HeLa cells were transfected with indicated expression vectors. PML acetylation was analyzed as in Fig. 1*B* except for the use of anti-HA antibody (*ab*) instead of anti-PML antibody for IP and IB. The lysates were also subjected to SDS-PAGE followed by autoradiography to confirm successful induction of histone acetylation by p300-HAT cotransfection. A representative autoradiograph of PML (*top panel*), the corresponding image of IB with anti-HA antibody (*second panel from the top*), and the autoradiograph of histone (*third panel from the top*) are presented. ^{14}C incorporation into PML and the amount of immunoprecipitated (*IP*) PML protein were quantified using analyzer of each imaging system. Relative ^{14}C incorporation adjusted by the efficiency of immunoprecipitation was calculated. The average and standard deviations for two independent analyses are presented (*bottom panel*). *B*, PML acetylation is increased in response to TSA treatment. HeLa cells were transfected with indicated expression vectors and treated with or without 10 μM TSA for 4 h. PML acetylation was analyzed and presented as in *A*. *WB*, Western blotting.

Next, we investigated the effect of PML sumoylation on PML-mediated apoptosis in response to TSA. Cotransfection of expression vectors for SUMO and Ubc9 further sensitized PML W transfectants to TSA-induced apoptosis (Fig. 5*C*, *third* and *fourth lanes*), whereas the proapoptotic effects of SUMO and Ubc9 were greatly reduced in control and PML M transfectants (Fig. 5*C*, *first* and *second lanes* and *fifth* and *sixth lanes*). Enhanced sumoylation of PML W induced by TSA and impaired sumoylation of PML M were observed also in PML$^{-/-}$ MEFs (Fig. 5*D*). These results suggest that sumoylation enhances PML-mediated apoptosis in response to TSA. To test this hypothesis, we created an expression vector for the PML-3K mutant, which had lysine-to-arginine mutations at all three PML sumoylation sites and cannot be sumoylated (22). Overexpression of PML-3K in either the presence or absence of SUMO and Ubc9 had little or no effect on TSA-induced apoptosis (Fig. 5*C*, *seventh* and *eighth lanes*), indicative of a requirement for PML sumoylation in TSA-mediated apoptosis. These results suggest the hypothesis that enhanced PML sumoylation through PML acetylation is one of the mechanisms of TSA-induced apoptosis.

Finally, to investigate the generality of the effects of TSA on PML among HDAC inhibitors, we used depsipeptide, another HDAC inhibitor that belongs to a different class. Depsipeptide enhanced acetylation and sumoylation of PML, and its apoptotic effect was increased by PML expression similarly to TSA (supplemental Fig. S8). These results further support the hypothetical importance of PML acetylation in HDAC inhibitor-induced apoptosis.

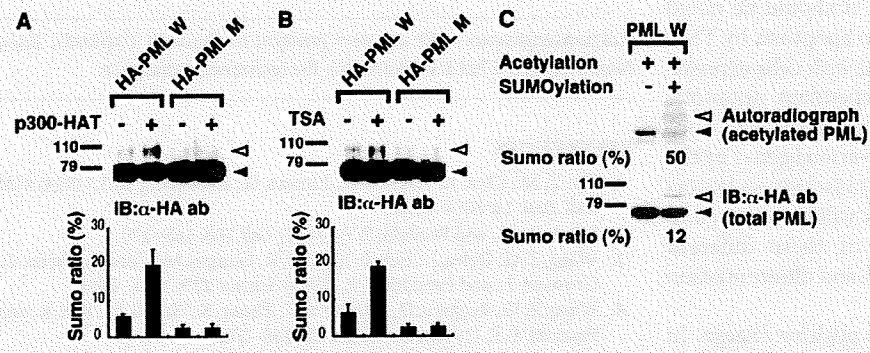

FIGURE 4. **PML acetylation is associated with enhanced sumoylation.** *A*, p300 coexpression enhances PML sumoylation. HeLa cells were transfected with the indicated expression vectors with cotransfection of those for SUMO and Ubc9. The cell lysates were subjected to SDS-PAGE followed by immunoblotting (*IB*) with anti-HA antibody (*ab*). The positions of sumoylated PML detected as an upper shifted band and nonsumoylated PML are indicated by *white* and *black arrowheads*, respectively. The ratios of sumoylated PML to total (sumoylated and unsumoylated PML) were calculated (SUMO ratio) and presented as bar charts. *B*, PML sumoylation increases in response to TSA treatment. PML sumoylation was examined as in *A* except that cells were treated with 10 μM TSA for 4 h instead of cotransfection of p300-HAT. *C*, acetylated PML is preferentially sumoylated *in vitro*. HA-tagged PML protein synthesized *in vitro* was immunoprecipitated with anti-HA antibody and incubated with p300-HAT and [^{14}C]acetyl-CoA as in Fig. 2*A*. The protein was subjected to an *in vitro* sumoylation assay and SDS-PAGE and transferred to a polyvinylidene difluoride membrane. Sumoylation of total (acetylated and nonacetylated) PML was visualized by IB with anti-HA antibody (*lower panel*). The same membrane was also subjected to an autoradiography to visualize sumoylation of acetylated PML (*upper panel*). Sumoylated and nonsumoylated PML are indicated as in *A*. SUMO ratio in each panel were calculated and presented at the *bottom*.

DISCUSSION

The data presented here demonstrate that acetylation of PML may enhance its sumoylation and play an important role in the control of PML-dependent apoptosis in response to TSA exposure. Sumoylation of PML is necessary for NB formation (5, 10), and the apoptotic effects of PML may be dependent on NB formation (see Introduction). Given our findings that PML acetylation is associated with increased PML sumoylation, this sumoylation-dependent NB formation may represent one of the mechanisms by which PML acetylation can enhance apoptosis. This hypothesis is supported by our findings that coexpression of SUMO and Ubc9 enhances PML-dependent apoptosis by TSA, that acetylation-defective mutants of PML exhibit defects in sumoylation and apoptosis in response to TSA treatment, and that a sumoylation-impaired PML mutant (PML-3K) is

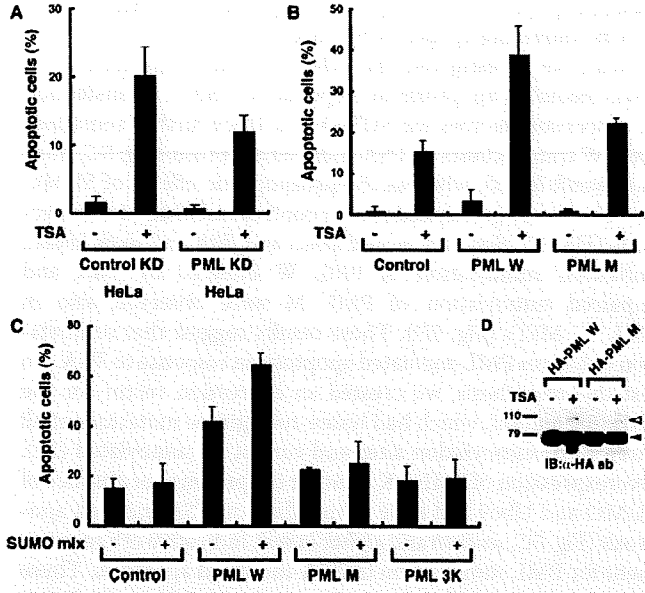

FIGURE 5. **PML acetylation is important for apoptosis induced by TSA.** *A*, PML knockdown reduces TSA-induced apoptosis in HeLa cells. HeLa cells whose PML was stably knocked down (PML KD HeLa) or control cells (Control KD HeLa) were treated with or without 1 μM TSA for 36 h. Apoptotic cells were detected and quantified as described under "Experimental Procedures." The ratios of apoptotic cells are plotted on bar charts. The averages of two independent analyses and standard deviations are shown. *B*, an acetylation-defective mutant of PML displayed impaired ability to mediate TSA-induced apoptosis. PML$^{-/-}$ MEFs were transfected with a bicistronic expression vector for GFP alone (control) or GFP and the indicated PML. GFP^{+} cells were sorted and treated with or without 1 μM TSA for 48 h. Apoptotic cells were analyzed as in *A*. *C*, coexpression of Ubc9 and SUMO enhances PML-mediated apoptosis in response to TSA. The analyses of apoptosis were performed as in *B* except that cells were cotransfected with expression vectors for SUMO and Ubc9 (SUMO mix) or an empty vector as indicated. *D*, increased PML sumoylation induced by TSA in PML$^{-/-}$ MEFs. PML sumoylation in PML$^{-/-}$ MEFs was examined as in Fig. 4*B*. *IB*, immunoblotting; *ab*, antibody.

also defective in TSA-mediated apoptosis. It should be noted that PML$^{-/-}$ MEF cells are still sensitive to apoptosis by TSA, although at a much reduced level compared with cells expressing PML. There may also be PML-independent apoptotic mechanisms that respond to TSA. This is not surprising, considering that TSA alters the expressions of various genes by the acetylation of histones and many kinds of transcription factors such as p53 (see Introduction). More work will be required to determine the individual contributions of these different actions of TSA on the proliferation, survival, and differentiation of cells.

Acetylation of lysine leads to loss of its positive charge. In some cases, arginine, a positive charged amino acid, and glutamine, a noncharged one, are reported to mimic nonacetylated and acetylated lysine, respectively. We examined whether glutamine substitution at acetylation sites, lysines 487 and 515, had an enhancing effect on PML sumoylation. The PML mutant with glutamine substitution, however, showed impaired sumoylation in HeLa cells similarly to the one with arginine substitution (data not shown). Effects of acetylation other than the loss of positive charge or subtle differences of amino acid structure between lysine and glutamine may be important for PML sumoylation.

Recent studies reveal that increasing numbers of proteins are targeted by both acetylation and sumoylation. However, the correlation between these modifications has hardly been investigated except the cases where both modifications competitively target the same lysine residue such as the cases of HIC1 (hypermethylated in cancer 1) and MEF2 (myocyte enhancer factor 2) (23, 24). This is the first report that suggests acetylation-dependent enhancement of sumoylation. Phosphorylation has been reported to regulate sumoylation. Recently, the classical sumoylation consensus motif (ψKXE) with an adjacent proline-directed phosphorylation motif (SP), ψKXEXXSP motif where ψ is a large hydrophobic residue and X is any residue, has been proposed as a phosphorylation-dependent sumoylation motif (25, 26). Between the two acetylation sites, lysines 487 and 515, lysine 487 is the major acetylation site, and K487R affects sumoylation more than K515R (Fig. 2, *B* and *C*, and data not shown). PML sumoylation is reported to occur at three lysine residues, lysine 65, 160, and 490 (22). It would be interesting to discover whether acetylation at lysine 487 specifically affects sumoylation at any of these lysine residues, especially at the adjacent lysine 490. p53 also has a similar sequence where an acetylated lysine lies adjacent to a sumoylated lysine (supplemental Fig. S9), although the correlation between acetylation and sumoylation has not been investigated (27). K$\psi\psi$KXE might be a motif of acetylation-dependent sumoylation.

In summary, our studies provide evidence for a new post-transcriptional modification of PML and a new mechanism of regulation of PML sumoylation, and establish a novel relationship between PML and TSA-induced apoptosis. This work provides new insights into the regulation of PML function and the control of protein sumoylation. Considering the large number of binding partners of PML and the key contributions of PML to the stability and function of the NBs, PML acetylation is likely to modulate multiple cell activities beyond apoptosis through regulation of recruitment or release of NBs components.

Acknowledgments—We are very grateful to Ryouhei Tanizaki, Yuka Nomura, and Chika Wakamatsu for technical assistance.

REFERENCES

1. Mu, Z. M., Chin, K. V., Liu, J. H., Lozano, G., and Chang, K. S. (1994) *Mol. Cell. Biol.* **14,** 6858–6867
2. Salomoni, P., and Pandolfi, P. P. (2002) *Cell* **108,** 165–170
3. Wang, Z. G., Delva, L., Gaboli, M., Rivi, R., Giorgio, M., Cordon-Cardo, C., Grosveld, F., and Pandolfi, P. P. (1998) *Science* **279,** 1547–1551
4. Wang, Z. G., Ruggero, D., Ronchetti, S., Zhong, S., Gaboli, M., Rivi, R., and Pandolfi, P. P. (1998) *Nat. Genet.* **20,** 266–272
5. Ishov, A. M., Sotnikov, A. G., Negorev, D., Vladimirova, O. V., Neff, N., Kamitani, T., Yeh, E. T., Strauss, J. F., III, and Maul, G. G. (1999) *J. Cell Biol.* **147,** 221–234
6. Dellaire, G., and Bazett-Jones, D. P. (2004) *Bioessays* **26,** 963–977
7. Dyck, J. A., Maul, G. G., Miller, W. H., Jr., Chen, J. D., Kakizuka, A., and Evans, R. M. (1994) *Cell* **76,** 333–343
8. Koken, M. H., Puvion-Dutilleul, F., Guillemin, M. C., Viron, A., Linares-Cruz, G., Stuurman, N., de Jong, L., Szostecki, C., Calvo, F., Chomienne, C., Degos, L., Puvion, E., and de Thé, H. (1994) *EMBO J.* **13,** 1073–1083
9. Weis, K., Rambaud, S., Lavau, C., Jansen, J., Carvalho, T., Carmo-Fonseca, M., Lamond, A., and Dejean, A. (1994) *Cell* **76,** 345–356
10. Zhong, S., Muller, S., Ronchetti, S., Freemont, P. S., Dejean, A., and Pandolfi, P. P. (2000) *Blood* **95,** 2748–2752

11. Kim, K. I., Baek, S. H., and Chung, C. H. (2002) *J. Cell. Physiol.* **191,** 257–268
12. Muller, S., Matunis, M. J., and Dejean, A. (1998) *EMBO J.* **17,** 61–70
13. Zhu, J., Koken, M. H., Quignon, F., Chelbi-Alix, M. K., Degos, L., Wang, Z. Y., Chen, Z., and de The, H. (1997) *Proc. Natl. Acad. Sci. U. S. A.* **94,** 3978–3983
14. Chen, G. Q., Shi, X. G., Tang, W., Xiong, S. M., Zhu, J., Cai, X., Han, Z. G., Ni, J. H., Shi, G. Y., Jia, P. M., Liu, M. M., He, K. L., Niu, C., Ma, J., Zhang, P., Zhang, T. D., Paul, P., Naoe, T., Kitamura, K., Miller, W., Waxman, S., Wang, Z. Y., de The, H., Chen, S. J., and Chen, Z. (1997) *Blood* **89,** 3345–3353
15. Niu, C., Yan, H., Yu, T., Sun, H. P., Liu, J. X., Li, X. S., Wu, W., Zhang, F. Q., Chen, Y., Zhou, L., Li, J. M., Zeng, X. Y., Yang, R. R., Yuan, M. M., Ren, M. Y., Gu, F. Y., Cao, Q., Gu, B. W., Su, X. Y., Chen, G. Q., Xiong, S. M., Zhang, T., Waxman, S., Wang, Z. Y., Chen, S. J., Hu, J., Shen, Z. X., and Chen, S. J. (1999) *Blood* **94,** 3315–3324
16. Marks, P. A., Richon, V. M., and Rifkind, R. A. (2000) *J. Natl. Cancer Inst.* **92,** 1210–1216
17. Wolffe, A. P., and Pruss, D. (1996) *Cell* **84,** 817–819
18. Glozak, M. A., Sengupta, N., Zhang, X., and Seto, E. (2005) *Gene (Amst.)* **363,** 15–23
19. Bandyopadhyay, D., Mishra, A., and Medrano, E. E. (2004) *Cancer Res.* **64,** 7706–7710
20. Terui, T., Murakami, K., Takimoto, R., Takahashi, M., Takada, K., Murakami, T., Minami, S., Matsunaga, T., Takayama, T., Kato, J., and Niitsu, Y. (2003) *Cancer Res.* **63,** 8948–8954
21. Hayakawa, F., and Privalsky, M. L. (2004) *Cancer Cell* **5,** 389–401
22. Kamitani, T., Kito, K., Nguyen, H. P., Wada, H., Fukuda-Kamitani, T., and Yeh, E. T. (1998) *J. Biol. Chem.* **273,** 26675–26682
23. Stankovic-Valentin, N., Deltour, S., Seeler, J., Pinte, S., Vergoten, G., Guerardel, C., Dejean, A., and Leprince, D. (2007) *Mol. Cell. Biol.* **27,** 2661–2675
24. Gregoire, S., and Yang, X. J. (2005) *Mol. Cell. Biol.* **25,** 2273–2287
25. Hietakangas, V., Anckar, J., Blomster, H. A., Fujimoto, M., Palvimo, J. J., Nakai, A., and Sistonen, L. (2006) *Proc. Natl. Acad. Sci. U. S. A.* **103,** 45–50
26. Yang, X. J., and Gregoire, S. (2006) *Mol. Cell* **23,** 779–786
27. Kwek, S. S., Derry, J., Tyner, A. L., Shen, Z., and Gudkov, A. V. (2001) *Oncogene* **20,** 2587–2599
28. Hayakawa, F., Towatari, M., Ozawa, Y., Tomita, A., Privalsky, M. L., and Saito, H. (2004) *J. Leukocyte Biol.* **75,** 529–540

bjh research paper

Clinical significance of nuclear non-phosphorylated beta-catenin in acute myeloid leukaemia and myelodysplastic syndrome

Jinglan Xu,[1] Momoko Suzuki,[1] Yousuke Niwa,[1] Junji Hiraga,[1] Tetsuro Nagasaka,[2] Masafumi Ito,[3] Shigeo Nakamura,[2] Akihiro Tomita,[1] Akihiro Abe,[1] Hitoshi Kiyoi,[4] Tomohiro Kinoshita[1] and Tomoki Naoe[1]

[1]Department of Haematology and Oncology, Nagoya University Graduate School of Medicine, Tsurumai-cho, Showa-ku, Nagoya, [2]Department of Clinical Pathophysiology, Nagoya University Graduate School of Medicine, Tsurumai-cho, Showa-ku, Nagoya, [3]Department of Pathology, Japanese Red Cross Nagoya 1st Hospital, Michishita-cho, Nakamura-ku, Nagoya, and [4]Department of Infectious Diseases, Nagoya University Hospital, Tsurumai-cho, Showa-ku, Nagoya, Japan

Received 5 June 2007; accepted for publication 11 September 2007

Correspondence: Jinglan Xu, Department of Haematology and Oncology, Nagoya University School of Medicine, 65 Tsurumai-cho, Showa-ku, Nagoya 466-8550, Japan. E-mail: xuj@med.nagoya-u.ac.jp

Summary

Wnt signaling activates the canonical pathway and induces the accumulation of non-phosphorylated beta-catenin (NPBC) in the nucleus. Although this pathway plays an important role in the maintenance of haematopoietic stem cells as well as in oncogenesis, the significance of nuclear NPBC remains unclear in malignant haematopoiesis. This study examined the expression of nuclear NPBC in bone marrow specimens from 54 and 44 patients with *de novo* acute myeloid leukaemia (AML) and myelodysplastic syndrome (MDS), respectively. On immunohistochemistry with an anti-NPBC antibody, the nuclei were positively stained in 22 and 18 of AML and MDS specimens, respectively. Staining of nuclear NPBC was associated with AML subtypes (M6 and M7), low complete remission (CR) rate, and poor prognosis. Nuclear NPBC was also associated with a high score when using the International Prognostic Scoring System (IPSS) for MDS and with −7/−7q and complex karyotypes. These findings suggest that *in situ* detection of nuclear NPBC by immunohistochemistry could provide new insights into the pathogenesis and prognosis of AML and MDS.

Keywords: beta-catenin, non-phosphorylated beta-catenin, acute myeloid leukaemia, myelodysplastic syndrome, immunohistochemistry.

The Wnt/beta-catenin pathway is involved in the self-renewal and proliferation of haematopoietic stem cells (Reya *et al*, 2003; Willert *et al*, 2003). Signaling is initiated by binding of Wnt proteins to transmembrane receptors of the Frizzeled family (Giles *et al*, 2003). In the absence of Wnt signals, a dedicated complex of proteins that includes the tumor suppressor gene product APC, axin, and glycogen synthase kinase-3-beta (GSK3-beta) phosphorylates specific serine and threonine residues within the N-terminal region of beta-catenin, which leads to the ubiquitination of beta-catenin and its degradation by proteasomes (Conacci-Sorrell *et al*, 2002; Noort *et al*, 2002; Staal *et al*, 2002; Giles *et al*, 2003). Wnt signals block GSK3beta activity, resulting in the accumulation of non-phosphorylated beta-catenin (NPBC), which is finally translocated to the nucleus (Noort *et al*, 2002; Staal *et al*, 2002). Nuclear NPBC interacts with T-cell transcription factor (TCF) and lymphoid enhancer factor (LEF), and it activates target genes such as *MYC* and *CCND1* (He *et al*, 1998; Tetsu & Maccormick, 1999). Therefore, nuclear NPBC is known to be oncogenic in many solid tumors (Bienz & Clevers, 2000; Polakis, 2000). Mutations of APC, beta-catenin, or axin, which are observed in various tumors, lead to stabilization of NPBC (Morin *et al*, 1997; Barker & Clevers, 2000).

In the bone marrow (BM), Wnt proteins activate the beta-catenin pathway and the non-obese severe combined immunodeficient (NOD-SCID)-repopulating capacity of normal haematopoietic stem cells. They lead to increased expression of *HOXB4* and *NOTCH1* implicated in the self-renewal of haematopoietic stem cells (Reya *et al*, 2003). Up-regulation of the beta-catenin pathway has been suggested in chronic myeloid leukaemia (CML)-derived granulocyte-macrophage progenitor cells (GMPs) and multiple myeloma (MM) cells (Derksen *et al*, 2004; Jamieson *et al*, 2004). Furthermore, beta-catenin reportedly plays a significant role in promoting cell proliferation, adhesion, and survival *in vitro* (Chung *et al*, 2002). The expression of beta-catenin is also enhanced by oncogenic FLT3 signals and associated with poor prognosis (Tickenbrock *et al*, 2005; Ysebaert *et al*, 2006). However, there are some contradictory reports. Studies of conditional knock-out mice with a beta-catenin gene (*Ctnnb1*) deletion indicated that *Ctnnb1* is not indispensable for haematopoiesis (Cobas *et al*, 2004). Furthermore, an active form of *Ctnnb1* compromised haematopoietic stem cell maintenance and blocked differentiation in transgenic mice experiments (Simon *et al*, 2005). The role of the Wnt/beta-catenin pathway in malignant haematopoiesis therefore needs to be further elucidated.

According to previous studies, the expression of beta-catenin is associated with activation of the Wnt pathway as well as poor prognosis (Tickenbrock *et al*, 2005; Ysebaert *et al*, 2006). However, beta-catenin is associated not only with Wnt signaling but also with adherence junctions (Conacci-Sorrell *et al*, 2002). It is anchored to the cell inner surface membrane via cadherins. In normal bone marrow (BM), the vascular endothelium expresses a significantly higher amount of beta-catenin relative to the level in haematopoietic cells. Accordingly, immunohistochemical detection of nuclear NPBC would enable a better understanding of the role of beta-catenin in leukaemia.

This study investigated the subcellular localization of beta-catenin in BM specimens from acute myeloid leukaemia (AML) and myelodysplastic syndrome (MDS) patients using two anti-beta-catenin antibodies: one against C-terminal peptides and another against N-terminal non-phosphorylated peptides. The latter antibody detected nuclear NPBC, and positive staining for nuclear NPBC was associated with particular clinical characteristics of AML and MDS.

Materials and methods

Patient samples

For clinical samples, BM clots were obtained during routine diagnostic procedures. Beta-catenin expression was analyzed in BM specimens from patients newly diagnosed at the Nagoya University Hospital between 2000 and 2006 (Table I). The *de novo* AML patients consisted of 35 men and 19 women with a median age of 53 years (range, 20–81 years), and *FLT3* mutations were detected in seven of 22 patients with AML (31·8%). The MDS patients consisted of 28 men and 16 women with a median age of 57 years (range, 22–89 years). BM mononuclear cells were harvested by standard Ficoll/Paque density gradient centrifugation (Amersham Pharmacia Biosciences, Roozendaal, the Netherlands), and were suspended in RPMI 1640 medium supplemented with 10% fetal bovine serum, 100 IU/ml of penicillin G and 100 μg/ml of streptomycin.

Table I. Clinical characteristics of AML and MDS patients according to nuclear NPBC expression.

	Nuclear NPBC$^+$	Nuclear NPBC$^-$	*P*-value
Patients with *de novo* AML	22	32	
Age (median)	54 (20–81)	53 (18–71)	NS
Sex/male/female	18/4	17/15	0·005
Laboratory data			
WBC ($\times10^9$/l; median)	3·5 (0·8–92·5)	5·3 (0·7–202·1)	NS
Hb (g/l; median)	74 (43–134)	98 (36–141)	0·01
PLT ($\times10^9$/l; median)	7·6 (0·3–170)	4·2 (1·1–27·3)	NS
PB blasts (%; median)	24 (0–82)	39 (0–99)	NS
BM blasts (%; median)	46·2 (20–86·5)	77·5 (29–98)	0·02
CR rate	13/22 (59·1%)	24/27 (88·9%)	0·01
Relapse rate	16/21 (76·2%)	14/24 (58·3%)	0·03
Patients with MDS	18	26	
Age	59 (26–76)	57 (22–89)	
Sex/male/female	12/6	16/10	0·05
Laboratory data			
WBC ($\times10^9$/l; median)	2·9 (1·2–9·0)	2·6 (1·6–5·9)	NS
Hb (g/l; median)	75 (46–151)	85 (47–127)	NS
PLT ($\times10^9$/l; median)	79 (7–122)	44 (7–400)	NS
BM blasts (%; median)	3 (0–30)	5 (0–30)	NS
IPSS score*			
Low risk	0	4	NS
Intermediate-1	4	12	NS
Intermediate-2	4	4	NS
High risk	3	1	0·04

NPBC, non-phosphorylated beta-catenin; AML, acute myeloid leukaemia; MDS, myelodysplastic syndrome; WBC, white blood cell count; Hb, hemoglobin concentration; PLT, platelet count; PB, peripheral blood; BM, bone marrow; CR, complete remission; IPSS, International Prognostic Scoring System.
*Full data was available in 32 of the 44 patients with MDS.

Antibodies

For immunohistochemical and immunoblot studies, two monoclonal antibodies were used; one was against C-terminal peptides (clone14, IgG1; BD Transduction Laboratories/Life Science Research, Heidelberg, Germany), enabling recognition of pan beta-catenin (PBC), and the other was against

N-terminal-peptides (clone 8E4, IgG1; Alexis Biochemicals, Lausanne, Switzerland), enabling recognition of NPBC.

Immunohistochemical staining

Samples were fixed with ice-cold 4% paraformaldehyde for 16–24 h, embedded in paraffin, sectioned transversely (thickness, 3 μm), and processed for immunohistochemistry to determine the localization of beta-catenin. After removal of paraffin with xylene and dehydration with a series of ethanol solutions, the tissue sections were subjected to microwave irradiation (750 W) for 15 min in 0·01 mol/l citrate buffer (pH 6·0). The sections were then placed in an automated immunostainer (Ventana Medical Systems, Tucson, AZ, USA) as described (Xu *et al*, 2002). For negative controls, primary antibodies were replaced with mouse IgG. The subcellular distribution of beta-catenin (i.e. restriction to the nucleus or presence in the membrane) was assessed without knowledge of the French-America-British (FAB) subtypes, *FLT3* mutations or karyotypes. We investigated a single case twice for NPBC expression. The entire section was screened to find the region with the highest immunostaining. The score was determined in each case after counting at least 500 nuclei in 3–5 randomly selected regions. When 20% or more of the BM mononuclear cells were positive for nuclear staining of NPBC, they were classified as nuclear NPBC$^+$. The cut-off value of 20% was determined by the median distribution of the percentage of BM mononuclear cells stained by NPBC. As described in the results, some erythroblasts were positive for NPBC but the number was <20% except in the case of M6 patients. On the other hand, almost all blasts in M7 and other cases tested positive. The discrimination of cell types based on the 20% criterion therefore enabled a clear delineation.

Immunoblotting

Cell lysates from AML cells were extracted as previously described (Ozeki *et al*, 2004). A total of 1×10^6 cells were directly lysed in sample buffer and then subjected to sodium dodecyl sulphate-polyacrylamide gel electrophoresis on a 10% gel, and the separated proteins were transferred to a polyvinylidene difluoride membrane (Bio-Rad, Hercules, CA, USA). The membrane was initially incubated at room temperature for 1 h with 5% nonfat milk and 0·1% Tween-20 in Tris-buffered saline and then overnight with mouse monoclonal antibodies at a 1:2000 dilution in the same solution. After washing, the membrane was incubated for 1 h with a 1:5000 dilution of horseradish peroxidase-conjugated mouse antibodies to mouse IgG (MBL, Amersham, Bucks, UK), and immune complexes were then detected with enhanced chemiluminescence (ECL) reagents (Amersham).

Statistical analysis

The χ^2 test was used to calculate the difference of frequencies between nuclear NPBC$^+$ and NPBC$^-$ groups. The Mann–Whitney *U*-test was used to compare continuous variables. Kaplan–Meier curves were drawn using STATVIEW software (Macintosh; SAS Institute, Cary, NC, USA). *P*-values <0·05 were considered significant.

Results

Using an anti-beta-catenin C-terminal peptide antibody, beta-catenin was stained in the membrane and cytoplasm of erythroid cells from normal BM. In *de novo* AML specimens, significant staining was observed only in M6. This antibody also detected BM vessels whose density was increased in AML specimens as previously reported (Serinsöz *et al*, 2004; Fig 1A). On the other hand, an anti-N-terminal nonphosphorylated peptide antibody gave no significant staining in the normal BM. In AML specimens, nuclear NPBC was detected in erythroid blasts, megakaryoblasts and some myeloblasts (Fig 1A). In M6 specimens, nuclear NPBC was detected in 30–80% of myelomonocytic cells and nearly 100% of erythroblastic cells (Fig 1A). In M7 specimens, megakaryocytes were also strongly positive for nuclear NPBC (Fig 1A). In total, 20% or more of the BM mononuclear cells were positive for nuclear NPBC in 22 (40·7%) of 54 AML patients (Table I, Fig 1B). There was a strong male predominance of nuclear NPBC$^+$ cases, comprising 81·8% (18/22) in AML patients (Table I). However, the reason for this is unclear. In our cohort study, the karyotypes of female patients correlated to t(8;21)/t(15;17), which did not express nuclear NPBC. Thus the small numbers of studied patients seem to give some bias to the male predominance. A large-scale study is necessary to confirm this association. Nuclear NPBC$^+$ staining was closely associated with AML subtype: it occurred frequently (8/9) in M6 and M7 and rarely (0/7) in M3 (Fig 1B), and nuclear NPBC$^+$ was preferentially detected in erythroid and megakaryoblastic leukaemia compared to other myeloid leukaemias (M6–M7 vs. M0–M5, $P < 0·001$).

In MDS specimens, erythroid cells and endothelial cells were stained with the anti-beta-catenin C-terminal peptide antibody (Fig 2A). As observed for AML specimens, the cytoplasm and inner membrane were stained by this antibody. The anti-beta-catenin N-terminal nonphosphorylated peptide antibody detected nuclear staining in myeloblasts and erythroblasts that was similar to the pattern seen in AML cases (Fig 2A). Nuclear NPBC was found in 18 (40·9%) of 44 MDS patients, and was related to the FAB classification of MDS (Table I, Fig 2B). Nuclear NPBC$^+$ was preferentially detected in refractory anaemia with excess blasts in transformation (RAEBT) compared to other MDS subtypes [RAEBT *versus* refractory anaemia (RA)/refractory anaemia with ringed sideroblasts (RARS)/RAEB, $P = 0·01$].

To confirm whether these two antibodies recognized beta-catenin, a total of 41 samples from AML and MDS patients were subjected to immunoblot analysis. The anti-beta-catenin C-terminal peptide antibody detected bands at a molecular weight of 95 kDa, corresponding to beta-catenin, in most

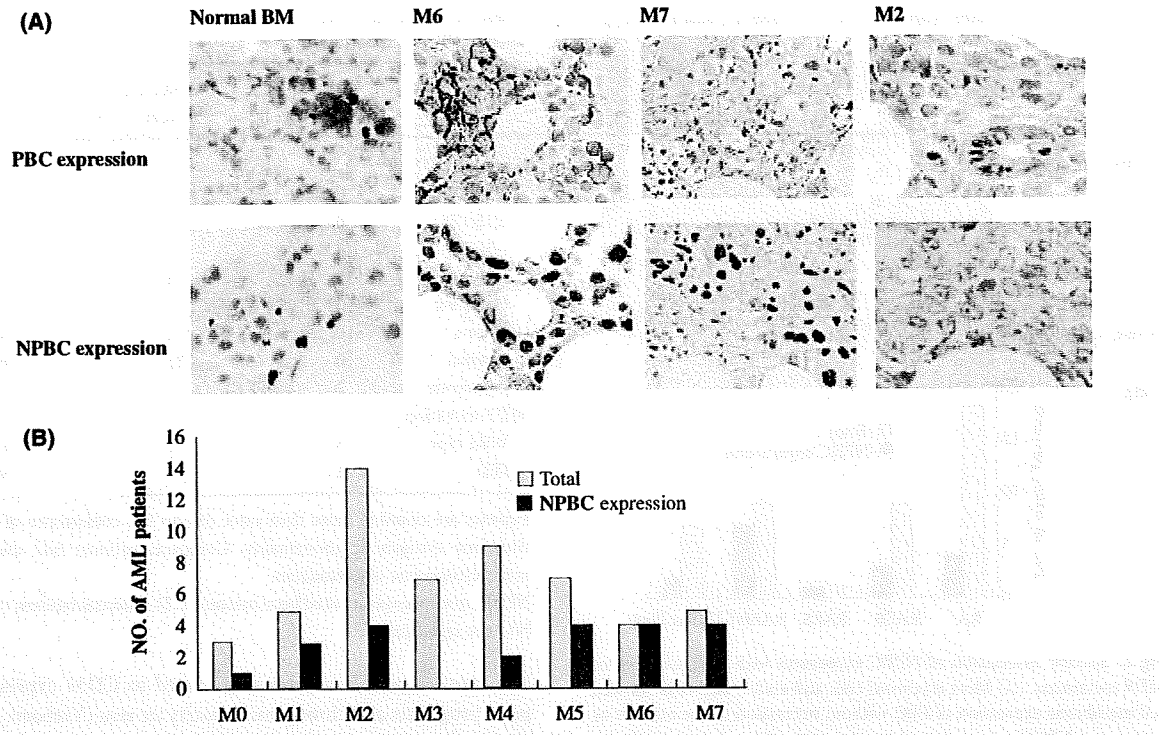

Fig 1. Specific association of NPBC expression with FAB subtypes of AML specimens. (A) In normal BM clots, PBC is expressed on the membranes of erythroid cells as well as endothelial cells. NPBC was not detected in normal BM clots. Most erythroid cells and endothelial cells showed cell membrane expression of PBC without expression in the nucleus or cytoplasm. NPBC was expressed in leukemia cells and was always restricted to the nucleus, especially in M6 and M7 specimens. Prominent staining of endothelial cells was seen in the vascular tissue in BM derived from an M2 patient with, though NPBC staining was negative in the same specimen. Original magnification ×40. (B) The graph presents data based on nuclear NPBC staining in paraffin sections from 54 patients with AML.

samples except for M3 (Fig 3A). The anti-N-terminal nonphosphorylated peptide antibody gave bands of the same size in only a few samples of AML and MDS (Fig 3B). The results of immunoblotting corresponded to those of immunostaining, although the latter was more sensitive than the former.

The above findings suggest that expression of nuclear NPBC could be used to identify some subsets of AML and MDS. Next we studied whether nuclear NPBC was associated with chromosomal abnormalities or genetic alterations. Previous studies suggested that AML-associated translocations, such as t(8;21) and t(15;17), contributed to the activation of gamma-catenin, or that *FLT3* mutation might be associated with the stabilization of beta-catenin. In this study, however, nuclear NPBC was never detected in AML with t(8;21) or t(15;17). In AML/MDS with −7/−7q and a complex karyotype, nuclear NPBC was frequently detected ($P = 0{\cdot}007$ and $P = 0{\cdot}02$, respectively; Table II). Moreover, detection was not related to *FLT3* internal tandem duplication (ITD; Table II).

Finally, we studied whether clinical characteristics and outcome were different between nuclear $NPBC^+$ and $NPBC^-$ AML patients. $NPBC^+$ AML patients showed significantly lower hemoglobin levels, lower blast percentages in the BM, and lower CR rates (Table I). There were no significant differences between the $NPBC^+$ and $NPBC^-$ groups in the MDS patients (Table I). However, nuclear NPBC was associated with a high International Prognostic Scoring System (IPSS) score (Table I). Of note, nuclear $NPBC^+$ AML patients had worse overall survival than $NPBC^-$ AML patients (Fig 4A). Even if the M6/M7 subtype and/or M3 subtype was excluded from the analysis, there was still a significant association between nuclear $NPBC^+$ and survival (Fig 4B–D).

Discussion

This study used nuclear NPBC as a biomarker for the activated Wnt/beta-catenin signaling pathway. The anti-beta-catenin C-terminal peptide antibody detected total beta-catenin in immunoblots but mainly cytoplasmic and membrane-associated beta-catenin in immunohistological analysis, whereas the anti-beta-catenin N-terminal nonphospholylated peptide antibody detected only nuclear beta-catenin in both analyses (data not shown). Accordingly, it was concluded that the nuclear staining with the latter antibody identified nuclear non-phosphorylated beta-catenin. Nuclear NPBC was detected in 22 (40·7%) of 54 AML patients and 18 (40·9%) of 44 MDS patients. Positive staining of nuclear NPBC was associated with particular AML subtypes (M6 and M7), a low complete remission rate, and poor prognosis. The presence of nuclear

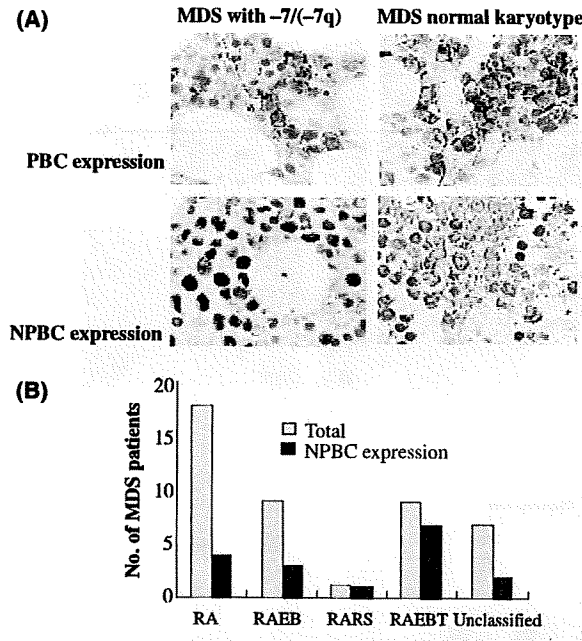

Fig 2. Specific association of NPBC expression with FAB subtypes of MDS specimens. (A) Most erythroid cells and endothelial cells showed cell membrane expression of PBC without expression in the nucleus or cytoplasm. NPBC was expressed in erythroid cells and was always restricted to the nucleus, especially in refractory anaemia with excess blasts in transformation (RAEBT) and MDS specimens with –7/–7(q). Original magnification ×40. (B) The graph presents data obtained for nuclear NPBC staining in paraffin sections from 44 patients with MDS. RA, refractory anaemia; RARS, RA with ringed sideroblasts; RAEB, RA with excess blasts.

NPBC was also associated with a high IPSS score of MDS and with –7/–7q and complex karyotypes.

Previous reports indicated that a significant proportion of AML samples expressed beta-catenin on immunoblot analysis.

Table II. Cytogenetic abnormalities and *FLT3* mutation according to nuclear NPBC expression.

	Nuclear NPBC$^+$ (*N*)	Nuclear NPBC$^-$ (*N*)	*P*-value
Karyotypes			
t(8;21)	0	3	NS
t(15;17)	0	4	NS
–5/–5q	4	1	NS
–7/–7q	12	6	0·007
Complex	13	7	0·02
Others	19	2	NS
Normal	10	31	0·0003
Unknown	7	1	0·02
FLT3 mutation			
Wild type	3	12	0·006
ITD	2	5	NS

Patients are counted more than once due to the coexistence of more than one cytogenetic abnormality. Complex patients had three or more cytogenetic abnormalities.
NPBC, non-phosphorylated beta-catenin; ITD, internal tandem repeat; NS, not significant.

The expression of beta-catenin is related to CD34 expression, poor prognosis and clonogenic capacity *ex vivo* (Ysebaert *et al*, 2006). Furthermore, beta-catenin is expressed in normal CD34$^+$ progenitor cells and the expression level is reduced upon differentiation (Simon *et al*, 2005). In these studies, however, the total beta-catenin level was analyzed only by immunoblot analysis. Beta-catenin is expressed not only as nuclear NPBC but also as a cadherin-associated protein in the inner cytomembrane (Conacci-Sorrell *et al*, 2002). The present study found that normal erythroblasts expressed cytoplasmic or membrane-associated beta-catenin but not nuclear NPBC (Fig 1A). Both membrane-associated and nuclear beta-catenin was expressed in malignant erythroblasts in subtype M6

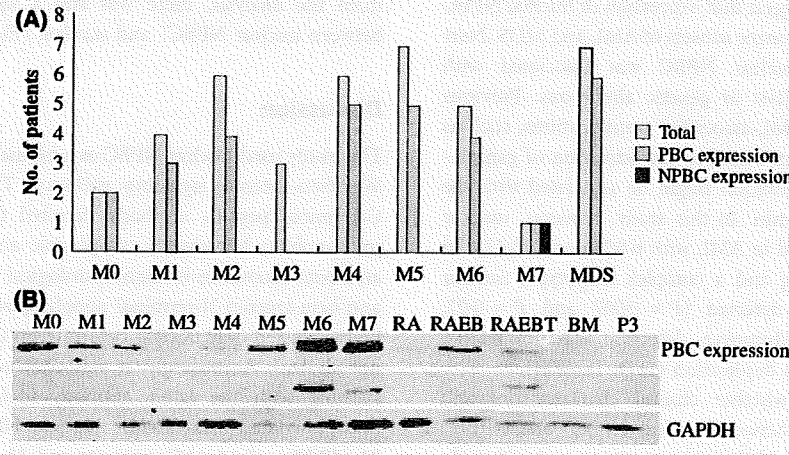

Fig 3. Beta-catenin expression of AML cells assessed by immunoblotting. (A) The graph shows data obtained for the expression of NPBC in mononuclear cells from 41 patients with AML, and the data indicate that expression of NPBC is specific to some FAB subtypes, especially to M6 and M7. (B) Representative immunoblots for PBC and NPBC in AML samples. RA, refractory anaemia; RARS, RA with ringed sideroblasts; RAEB, RA with excess blasts; RAEBT, refractory anaemia with excess blasts in transformation.

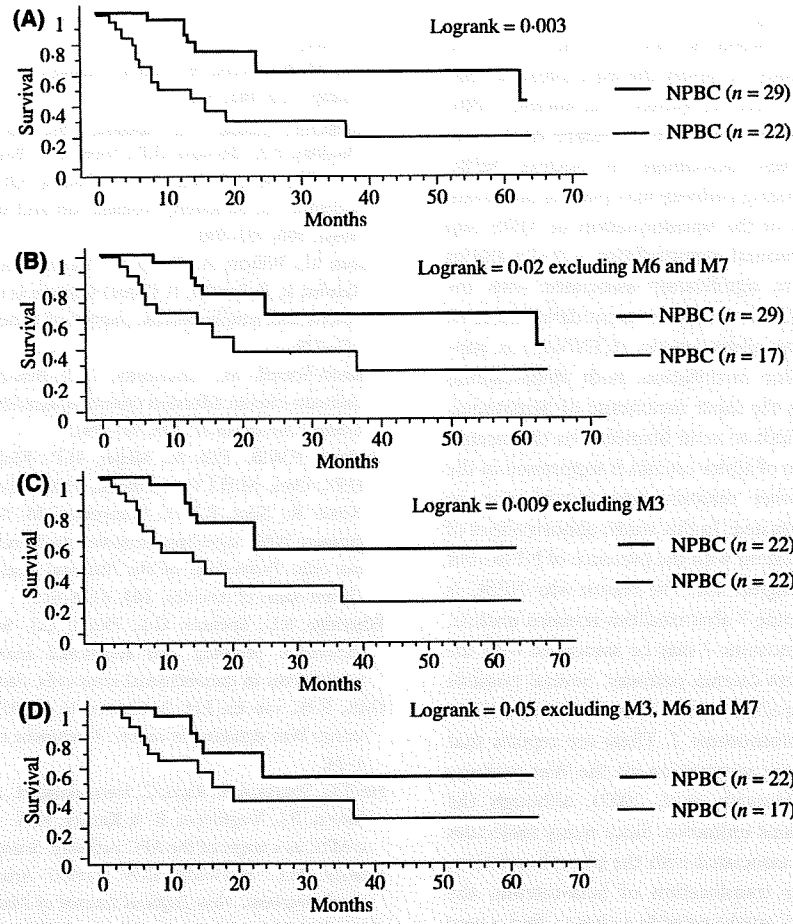

Fig 4. Kaplan–Meier cumulative survival curves were calculated for 51 AML patients (A) and 46 patients excluding subtype M6/M7 (B), 44 patients excluding subtype M3 (C), 39 patients excluding subtype M3/M6/M7 (D), respectively, according to the presence of nuclear NPBC. Comparison of the survival curves using the log-rank test identified nuclear NPBC$^+$ as a prognostic factor.

(Fig 1A). These findings suggest that increased nuclear NPBC levels were the result of aberrant signal transduction in the Wnt pathway or an abnormality of beta-catenin itself.

In this study, the expression levels of total and non-phosphorylated beta-catenin were correlated but varied significantly among leukemia samples. In M6 and M7 samples, the expression of beta-catenin was significantly augmented, whereas it was hardly detected in M3 and normal BM samples. These variations suggest the possibility that Wnt/beta-catenin signaling is mediated by multiple factors, such as immaturity, lineage, and oncogenic signals.

We established a correlation between nuclear NPBC$^+$ and poor survival in AML patients. The prognostic value of total beta-catenin expression has been previously studied in AML patients (Ysebaert *et al*, 2006), but the present study clearly showed for the first time that nuclear NPBC is associated with prognosis. The association was still observed even if M6/M7 and/or M3 patients were excluded from the analysis. Nuclear NPBC might be a new prognostic marker for AML and MDS that can be evaluated by histopathological examination.

Wnts are a family of paracrine and autocrine factors that regulate cell growth and cell fate (Reya *et al*, 2003). The Wnt autocrine signaling mechanism was initially discovered in human breast and ovarian tumor cell lines as well as in MM primary samples (Bafico *et al*, 2004; Derksen *et al*, 2004). Since several Wnt family members have been reported in BM stromal cells, it is possible that leukaemia cells respond to different proteins of the Wnt/beta-catenin pathway secreted by stromal cells in a paracrine fashion (Austin *et al*, 1997; Van Den Berg *et al*, 1998; Etheridge *et al*, 2004). Nuclear NPBC was detected in some cell lines only when they were transplanted in non-obese diabetic/severe combined immunodeficient/gammacnull (NOG) mice (data not shown). Thus, the leukaemia niche may have an important role in nuclear NPBC expression during AML.

MDS is a clonal hematopoietic stem cell disorder characterized by multi-lineage dysplasia and pancytopenia in which further genetic events may be required for the rapid expansion of leukaemic blasts (Heaney & Golde, 1999; Hirai, 2003). Although nuclear NPBC has been studied in many cancers as

well as haematological malignancies, it has not been studied in MDS (Morin *et al*, 1997; Barker & Clevers, 2000; Giles *et al*, 2003). This is the first study to report the expression of beta-catenin in MDS patients. Here we showed that nuclear NPBC was related to the IPSS score and that secondary AML from MDS showed the highest percentage of nuclear NPBC expression. The Wnt signaling pathway may play an important role in the pathogenesis of the transformation of MDS into AML. Regarding chromosomal abnormalities, −7/−7q and/or complex karyotypes were significantly associated with the presence of nuclear NPBC. According to recent data (Liu *et al*, 2006), the gene encoding alpha-catenin (*CTNNA1*) is suppressed by deletion and/or methylation. Both alpha-catenin and beta-catenin bind to the inner membrane of hematopoietic cells, and cadherin binds to actin filaments via the catenin complex. If the expression of alpha-catenin is suppressed in the 5q- genotype or for other reasons, beta-catenin may be abnormally located or activated. In this study, abnormalities of chromosome 5 were associated with the presence of NPBC but this was not statistically significant. The reason why NPBC is associated with chromosome 7 abnormalities remains unclear. A gene encoded by chromosome 7 may be associated with the regulation of the Wnt/beta-catenin pathway. Several possible candidate genes including *SFRP4*, *WNT2*, and *FZD1* and *FZD9* are located at human chromosome 7. There are reports that sFRP4 plays a role in tumor suppression via the Wnt pathway (Hrzenjak *et al*, 2004; Horvath *et al*, 2007), although the specific relationship remains unknown. Since many molecules are directly or indirectly associated with the phosphorylation, stabilization and nuclear translocation of beta-catenin, the presence of nuclear NPBC might provide a clue to find a new leukemia-associated signaling mechanism.

In conclusion, *in situ* detection of nuclear NPBC by immunohistochemistry of paraffin sections from BM specimens could be used to predict the prognosis of AML and MDS. Understanding the mechanisms leading to leukemogenesis in nuclear NPBC$^+$ AML and MDS may lead to new anti-leukemia therapies.

Acknowledgements

This study is partly supported by Grants-in-Aid from National Institute of Biomedical Innovation and from Ministry of Education, Culture, Sports, Science and Technology on the Scientific Research. We thank Kazuko Matsuba for technical assistance, and Mari Otsuka for secretarial assistance.

References

Austin, T.W., Solar, G.P., Ziegler, F.C., Liem, L. & Matthews, W. (1997) A role for the Wnt gene family in hematopoiesis: expansion of multilineage progenitor cells. *Blood*, **89**, 3624–3635.

Bafico, A., Liu, G., Goldin, L., Harris, V. & Aaronson, S.A. (2004) An autocrine mechanism for constitutive Wnt pathway activation in human cancer cells. *Cancer Cell*, **6**, 497–506.

Barker, N. & Clevers, H. (2000) Catenins, wnt signaling and cancer. *BioEssays*, **22**, 961–965.

Bienz, M. & Clevers, H. (2000) Linking colorectal cancer to Wnt signaling. *Cell*, **103**, 311–320.

Chung, E.J., Hwang, S.G., Nguyen, P.M., Lee, S., Kim, J.S., Kim, J.W., Henkart, P.A., Bottaro, D.P., Soon, L.L., Bonvini, P., Lee, S.J., Karp, J.E., Oh, H.J., Rubin, J.S. & Trepel, J.B. (2002) Regulation of leukemic cell adhesion, proliferation and survival by beta-catenin. *Blood*, **100**, 982–990.

Cobas, M., Wilson, A., Ernst, B., Mancini, S.J.C., MacDonald, H.R., Kemler, R. & Radtke, F. (2004) Catenin is dispensable for hematopoiesis and lymphopoiesis. *Journal of Experimental Medicine*, **199**, 221–229.

Conacci-Sorrell, M., Zhurinsky, J. & Ben-ZeÅfev, A. (2002) The cadherin-catenin adhesion system in signaling and cancer. *Journal of Clinical Investigation*, **109**, 987–991.

Derksen, P.W.B., Tjin, E., Meijer, H.P., Klok, M.D., Mac Gillavry, H.D., Oers, M.H.J.V., Lokhorst, H.M., Bloem, A.C., Clevers, H., Nusse, R., Neut, R.V.D., Spaargaren, M. & Pals, S.T. (2004) Illegitimate WNT signaling promotes proliferation of multiple myeloma cells. *Proceedings of the National Academy of Sciences of the United States of America*, **101**, 6122–6127.

Etheridge, S.L., Spencer, G.J., Heath, D.J. & Genever, P.G. (2004) Expression profiling and functional analysis of wnt signaling mechanisms in mesenchymal stem cells. *Stem Cells*, **22**, 849–860.

Giles, R.H., van Es, J.H. & Clevers, H. (2003) Caught up in a Wnt storm: Wnt signaling in cancer. *Biochimica et Biophysica Acta*, **1653**, 1–24.

He, T.C., Sparks, A.B., Rago, C., Hermeking, H., Zawel, L., da Costa, L.T., Morin, P.J., Vogelstein, B. & Kinzler, K.W. (1998) Identification of c-MYC as a target of the APC pathway. *Science*, **281**, 1509–1512.

Heaney, M.L. & Golde, D.W. (1999) Articles medical progress: myelodysplasia. *New England Journal of Medicine*, **340**, 1649–1660.

Hirai, H. (2003) Molecular mechanisms of myelodysplastic syndrome. *Japanese Journal of Clinical Oncology*, **33**, 153–160.

Horvath, L.G., Lelliott, J.E., Kench, J.G., Lee, C.S., Williams, E.D., Saunders, D.N., Grygiel, J.J., Sutherland, R.L. & Henshall, S.M. (2007) Secreted frizzled-related protein 4 inhibits proliferation and metastatic potential in prostate cancer. *Prostate*, **67**, 1081–1090.

Hrzenjak, A., Tippl, M., Kremser, M.L., Strohmeier, B., Guelly, C., Neumeister, D., Lax, S., Moinfar, F., Tabrizi, A.D., Isadi-Moud, N., Zatloukal, K. & Denk, H. (2004) Inverse correlation of secreted frizzled-related protein 4 and -catenin expression in endometrial stromal sarcomas. *The Journal of Pathology*, **204**, 19–27.

Jamieson, C.H.M., Ailles, L.E., Dylla, S.J., Muijtjens, M., Jones, C., Zehnder, J.L., Gotlib, J., Li, K., Manz, M.G., Keating, A., Sawyers, C.L. & Weissman, I.L. (2004) Granulocyte-macrophage progenitors as candidate leukemic stem cells in blast-crisis CML. *New England Journal of Medicine*, **351**, 657–667.

Liu, T.X., Becker, M.W., Jelinek, J., Wu, W.S., Deng, M., Mikhalkevich, N., Hsu, K., Bloomfield, C.D., Stone, R.M., DeAngelo, D.J., Galinsky, I.A., Issa, J.P., Clarke, M.F. & Look, A.T. (2006) Chromosome 5q deletion and epigenetic suppression of the gene encoding -catenin (CTNNA1) in myeloid cell transformation. *Nature Medicine*, **13**, 78–83.

Morin, P.J., Sparks, A.B., Korinek, V., Barker, N., Clevers, H., Vogelstein, B. & Kinzler, W.K. (1997) Activation of beta-catenin-Tcf signaling in colon cancer by mutations in beta-catenin or APC. *Science*, **275**, 1787–1790.

Noort, M.V., Meeldijk, J., Zee, R.V.D., Destree, O. & Clevers, H. (2002) Wnt signaling controls the phosphorylation status of beta-catenin. *Journal of Biological Chemistry*, **277**, 17901–17905.

Ozeki, K., Kiyoi, H., Hirose, Y., Iwai, M., Ninomiya, M., Kodera, Y., Miyawaki, S., Kuriyama, K., Shimazaki, C., Akiyama, H., Nishimura, M., Motoji, T., Shinagawa, K., Takeshita, A., Ueda, R., Ohno, R., Emi, N. & Naoe, T. (2004) Biologic and clinical significance of the FLT3 transcript level in acute myeloid leukemia. *Blood*, **103**, 1901–1908.

Polakis, P. (2000) Wnt signaling and cancer. *Genes and Development*, **14**, 1837–1851.

Reya, T., Duncan, A.W., Ailles, L., Dome, J., Scherer, D.C., Willert, K., Hintz, L., Nusse, R. & Weissman, I.L. (2003) A role for Wnt signaling in self-renewal of hematopoietic stem cells. *Nature*, **423**, 409–414.

Serinsöz, E., Neusch, M., Büsche, G., Wasielewski, R.V., Kreipe, H. & Bock, O. (2004) Aberrant expression of beta-catenin discriminates acute myeloid leukaemia from acute lymphoblastic leukaemia. *British Journal of Haematology*, **126**, 313–319.

Simon, M., Grandage, V.L., Linch, D.C. & Khwaja, A. (2005) Constitutive activation of the Wnt/beta-catenin signalling pathway in acute myeloid leukaemia. *Oncogene*, **24**, 2410–2420.

Staal, F.J.T., Noort, M.V., Strous, G.J. & Clevers, H.C. (2002) Wnt signals are transmitted through N-terminally dephosphorylated beta-catenin. *EMBO Reports*, **3**, 63–68.

Tetsu, O. & Maccormick, F. (1999) Catenin regulates expression of cyclin D1 in colon carcinoma cells. *Nature*, **398**, 422–426.

Tickenbrock, L., Schwable, J., Wiedehage, M., Steffen, B., Sargin, B., Choudhary, C., Brandts, C., Berdel, W.E., Tidow, C.M. & Serve, H. (2005) Flt3 tandem duplication mutations cooperate with Wnt signaling in leukemic signal transduction. *Blood*, **105**, 3699–3706.

Van Den Berg, D.J., Sharma, A.K., Bruno, E. & Hoffman, R. (1998) Role of members of the Wnt gene family in human hematopoiesis. *Blood*, **92**, 3189–3202.

Willert, K., Brown, J.D., Danenberg, E., Duncan, A.W., Weissman, I.L., Reya, T., Yates, J.R. & Nusse, R. (2003) Wnt proteins are lipid-modified and can actas stem cell growth factors. *Nature*, **423**, 448–452.

Xu, J.L., Lai, R., Kinoshita, T., Nakashima, N. & Nagasaka, T. (2002) Proliferation, apoptosis and intratumoral vascularity in multiple myeloma: correlation with the clinical stage and cytologic grade. *Journal of Clinical Pathology*, **55**, 530–534.

Ysebaert, L., Chicanne, G., Demur, C., Toni, F.D., Houdellier, N.P., Ruidavets, J.B., Mas, V.M.D., Huguet, F.R., Laurent, G., Payrastre, B., Manenti, S. & Sultan, C.R. (2006) Expression of beta-catenin by acute myeloid leukemia cells predicts enhanced clonogenic capacities and poor prognosis. *Leukemia*, **20**, 1211–1216.

Int J Hematol (2008) 88:73–81
DOI 10.1007/s12185-008-0115-2

ORIGINAL ARTICLE

A safety, pharmacokinetic and pharmacodynamic investigation of deferasirox (Exjade®, ICL670) in patients with transfusion-dependent anemias and iron-overload: a Phase I study in Japan

Keisuke Miyazawa · Kazuma Ohyashiki · Akio Urabe · Tomoko Hata · Shinji Nakao · Keiya Ozawa · Takayuki Ishikawa · Junji Kato · Yoichi Tatsumi · Hiraku Mori · Midori Kondo · Junsuke Taniguchi · Hiromi Tanii · Lisa Rojkjaer · Mitsuhiro Omine

Received: 19 March 2008 / Revised: 26 April 2008 / Accepted: 29 May 2008 / Published online: 4 July 2008

Abstract The pharmacokinetics (PK) and pharmacodynamics (PD) of the once-daily, oral ironchelating agent, deferasirox (Exjade®, ICL670), have been evaluated further in a Phase I, openlabel, multicenter, dose-escalation study in Japanese patients with myelodysplastic syndromes, aplastic anemia, and other anemias. Deferasirox was initially administered as a single dose of 5 ($n = 6$), 10 ($n = 7$), 20 ($n = 6$) or 30 ($n = 7$) mg/(kg day) and then after 7 days seven daily doses were administered. Linear PK (C_{max} and AUC) were observed at all doses after a single dose and at steady state, and dose-dependent iron excretion was observed. Pharmacokinetic/pharmacodynamic parameters were similar to those reported in a Caucasian β-thalassemia cohort. Following the single- and multiple-dose phases, 21 of 26 patients progressed to a 3-year extension phase of the study, where dose reductions and increases [5–30 mg/(kg day)] were allowed following safety and efficacy assessments. In the interim, 1-year data show that deferasirox was well tolerated, with generally infrequent and mild adverse events. Reductions in serum ferritin levels were observed and a negative iron balance achieved at doses of 20–30 mg/(kg day). These data suggest that deferasirox has a stable and predictable PK/PD profile, irrespective of underlying disease or race, and a predictable and manageable safety profile suitable for chronic administration.

Keywords Iron chelation · Deferasirox · Iron overload · Myelodysplastic syndrome

K. Miyazawa (✉) · K. Ohyashiki
First Department of Internal Medicine (Hematology/Oncology), Tokyo Medical University, 6-7-1 Nishishinjuku, Shinjuku-ku, Tokyo 160-0023, Japan
e-mail: miyazawa@tokyo-med.ac.jp

A. Urabe
NTT Kanto Medical Center, Tokyo, Japan

T. Hata
Nagasaki University, Nagasaki, Japan

S. Nakao
Kanazawa University, Ishikawa, Japan

K. Ozawa
Jichi Medical University, Tochigi, Japan

T. Ishikawa
Kyoto University, Kyoto, Japan

J. Kato
Sapporo Medical University, Sapporo, Japan

Y. Tatsumi
Kinki University, Osaka, Japan

H. Mori · M. Omine
Showa University Fujigaoka Hospital, Yokohama, Japan

M. Kondo · J. Taniguchi · H. Tanii
Novartis Pharma K.K., Tokyo, Japan

L. Rojkjaer
Novartis Pharma A.G., Basel, Switzerland

1 Introduction

Blood transfusions provide key supportive therapy for patients with chronic anemias, relieving the disease symptoms, improving quality of life, and extending survival [1–3]. However, the senescence of transfused red blood cells leads to the release of excess iron for which the body has no active mechanism of removal. Once levels of transferrin, an iron-binding protein, are saturated, free iron begins to circulate and is taken up and stored in the

parenchymal cells of the liver, heart, endocrine organs, brain, and joints [4, 5]. The accumulation of toxic iron leads to the generation of active oxygen species, resulting in DNA damage, lipid peroxidation, apoptosis and, therefore, ongoing tissue damage. If iron levels remain uncontrolled, progressive organ dysfunction will result in death, principally from cardiac and liver failure. Iron overload can be effectively managed with iron chelation therapy, which can prevent the consequences of iron toxicity and improve patients' long-term outcomes [6–9].

In Japan, the myelodysplastic syndromes (MDS) and aplastic anemia (AA) are the most common anemias requiring regular blood transfusion therapy. Despite widespread recognition of the risks associated with iron overload, and the subsequent need to manage iron levels, treatment options are, at present, limited to deferoxamine (Desferal®, DFO), an iron chelator with a high molecular weight that requires parenteral administration. In contrast to most countries around the world where DFO is administered via slow subcutaneous infusion utilizing a portable pump because of its short half-life, DFO is approved in Japan only for intravenous and intramuscular administration. In contrast to the recommended regimen of slow subcutaneous infusion 5–7 nights/week, it is therefore a common practice for DFO to be administered only once every 2 weeks in a hospital setting. As studies have demonstrated that chelation coverage is limited to periods of drug exposure, infrequent infusions will allow raised levels of non-transferrin bound iron to reoccur, exposing patients to toxic iron levels [10, 11]. A recent survey on Japanese patients with MDS, AA, and other anemias, highlighted that less than half had received iron chelation therapy, and of those who were treated, less than 9% received continuous/daily DFO therapy [12]. A high mortality rate was noted in this population, primarily from cardiac and liver failure, conditions commonly associated with iron overload [5, 13]. Daily or continuous iron chelation therapy was seen to effectively reduce iron burden and improve organ function [12].

Once-daily oral therapy with deferasirox (Exjade®, ICL670) has the potential to overcome the limitations of DFO treatment, providing convenient therapy and 24-h chelation coverage [14]. Registration studies conducted on non-Japanese adult and pediatric patients have demonstrated a similar efficacy to DFO at comparable doses, and dose-dependent efficacy in reducing body iron burden across a wide range of transfusion-dependent anemias [15–18]. Deferasirox has since been approved in more than 85 countries worldwide. Here, we present the findings of a Phase I clinical trial on Japanese patients with transfusion-dependent anemias treated with deferasirox in an initial pharmacokinetic (PK)/pharmacodynamic (PD) study, and interim analyses of data from the subsequent extension phase. The PK/PD parameters were compared with those previously reported in a cohort of iron-overloaded Caucasian patients with β-thalassemia [19].

2 Methods

2.1 Study objectives

The primary objective was to evaluate the tolerability and safety of deferasirox in Japanese patients with transfusional iron overload. Secondary objectives were to evaluate the PK and PD of deferasirox, including iron excretion. A comparison of the PK/PD data with those of a previously published Phase I trial (study 0104) conducted on non-Japanese β-thalassemia patients was also performed [19].

2.2 Patients

Eligible patients were ≥20 years of age, with transfusion-dependent MDS, AA or other anemias (pure red cell aplasia: PRCA, myelofibrosis: MF), having received a lifetime history of ≥35 U of packed red blood cells (RBCs). In Japan, 1 U of RBCs contains 200 mL of whole blood, and provides approximately 100 mg of iron. Serum ferritin values ≥1,000 μg/L as confirmed by at least two evaluations, during the 4 weeks prior to enrollment and an ECOG performance value of 0–2 were required. As a result, the patient with chronic inflammation, for example adult Still disease or hemophagocytic syndrome, did not enroll in this study. Patients receiving DFO therapy during the 4 weeks prior to the start of deferasirox treatment were excluded. Other parameters that excluded patients from the study at screening included alanine aminotransferase (ALT) levels >250 U/L, serum creatinine levels above the upper limit of normal (ULN), a urinary protein/creatinine aplastic anemia ratio >0.5 mg/mg, serological evidence of chronic hepatitis B virus infection, clinical evidence of active hepatitis C virus infection, uncontrolled gastrointestinal problems (diarrhea, constipation, or bleeding), and cataract or a previous history of clinically relevant ocular dysfunction related to iron chelation. All patients provided written informed consent.

The study by Nisbet-Brown et al. [19] (Study 0104), which was used for comparison, enrolled Caucasian patients (male and female, aged ≥16 years) with β-thalassemia and transfusional iron overload.

2.3 Study design and dosing

This Phase I, collaborative, openlabel, non-blind, dose-escalation study was conducted in nine centers in Japan. The study was conducted in three phases, a single-dose phase (1-day treatment in each dose cohort), a multiple-dose

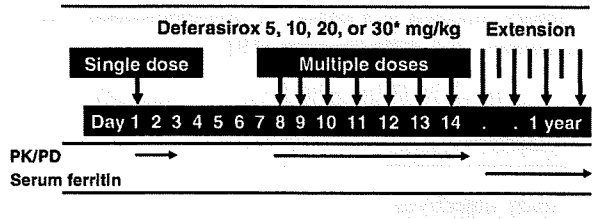

Fig. 1 Study design indicating dosing and PK/PD assessments. *Asterisk* denotes cohort commenced treatment on 20 mg/(kg day) in the extension

phase (7-day treatment in each dose cohort), and an extension phase (1-year data reported; Fig. 1). Single dosing was initiated with a cohort treated at 5 mg/kg. Efficacy and Safety Committee review subsequently approved enrollment of the next dosing cohort (10, 20, and 30 mg/kg) and progression to the multiple-dose phase where patients received daily doses of deferasirox 30 min before breakfast. Deferasirox dosing was based on previous studies in Caucasian populations [19, 20]. Patients were hospitalized during the single- and multiple-dose periods and given a standard low iron diet from day 1 to day 14. In study 0104, deferasirox was administered at 10, 20, and 40 mg/kg once daily for 12 days [19].

Following completion of the single- and multiple-dose phases of the study, treatment could continue into the extension phase for approximately 3 years at the patient's request in the ethical point of view for patient. Following Efficacy and Safety Committee review, a recommendation to adjust deferasirox dose in relation to transfusion requirement was made. As a result, patients receiving deferasirox 5, 10 or 20 mg/(kg day) continued into the extension phase at the same doses, but those who had originally received 30 mg/(kg day) began the extension phase on 20 mg/(kg day) to avoid potential over chelation. Dose adjustment was subsequently allowed to 30 mg/(kg day) in the extension phase following a trend of increasing serum ferritin levels or increased frequency of blood transfusion. Dose was decreased down to 5 mg/(kg day) in cases of increasing serum creatinine levels, adverse events (AEs) or decreases in serum ferritin level. Dose reduction or interruptions were implemented for skin rash, increase in serum creatinine, and increase in urinary protein/creatinine ratio. If serum ferritin fell to $\leq$500 μg/L on two consecutive study visits, treatment was interrupted until serum ferritin was >1,000 μg/L.

2.4 Safety assessments

Safety evaluations were based on reports of AEs and serious AEs, plus assessment of hematology, blood chemistry, urinalysis, vital signs, physical examinations, electrocardiograms, and ocular and audiometry examinations.

2.5 Pharmacokinetic/pharmacodynamic evaluation

Pharmacokinetic/pharmacodynamic assessments were made during the single- and multiple-dose phases. Pharmacokinetic calculations were based on free deferasirox and the iron-complex of deferasirox (Fe-[ICL670]$_2$) by means of a non-compartmental analysis to determine t_{max}, C_{max}, AUC_{0-24}, and $t_{1/2}$. Total iron excretion was calculated as the sum of the urinary and fecal iron excretion. Iron excretion induced by deferasirox was calculated as the difference between an average daily iron excretion during the treatment period (days 11, 12, 13, and 14) and an average daily iron excretion during the cessation period (days 5, 6, and 7) as the baseline value.

2.6 Markers of iron stores

During the extension phase, safety, serum ferritin, and blood biochemical tests [including albumin, alkaline phosphatase, total bilirubin, blood urea nitrogen (BUN), cholesterol, creatinine, γ-GTP, glucose, LDH, total protein, ALT, AST, triglycerides, uric acid, CRP, sodium, potassium, chloride, calcium, inorganic phosphorus, and magnesium] were evaluated monthly. Exploratory examination of changes from baseline in serum ferritin levels was conducted.

3 Results

3.1 Patient demographics

Twenty-six patients with MDS, AA or other anemias were enrolled in the single- and multiple-dose phases, all of whom completed the core phase of the study (Table 1). Twenty-one patients continued to the extension phase. Study 0104, which was used to compare the PK/PD results from the current study, enrolled nine male and nine female Caucasian patients with β-thalassemia with a median age of 26.4 years (range 18–39) [19], lower than the median age of 69.5 years (range 26–93) of the Japanese patients in the current study.

3.2 Dosing and exposure to deferasirox

All 26 patients completed the single- and multiple-dose phases. Of these 21 patients who wished to continue deferasirox treatment as extension phase, 14 (66.7%) remain on study treatment for 1 year and are continuing in the study. Those who withdrew did so primarily due to AEs or improvements in serum ferritin value that meant chelation therapy was no longer required (Table 2).

Adjustments to the starting dose were made due to insufficient efficacy of the initial dose as assessed by serum ferritin (increase in dose) and AEs (decrease in dose;

Table 1 Patient characteristics

	Deferasirox dose [mg/(kg day)]				
Core phase	5 ($n = 6$)	10 ($n = 7$)	20 ($n = 6$)	30 ($n = 7$)	Total ($n = 26$)
Median age, years (range)	71.5 (28–78)	68.0 (34–93)	66.0 (26–74)	75.0 (46–87)	69.5 (26–93)
Male:female	1:5	3:4	1:5	3:4	8:18
Underlying anemia, *n* (%)					
MDS	3 (50)	5 (71.4)	4 (66.7)	4 (57.1)	16 (61.5)
AA	3 (50)	1 (14.3)	1 (16.7)	1 (14.3)	6 (23.1)
Other anemias[a]	0	1 (14.3)	1 (16.7)	2 (28.6)	4 (15.4)

Extension phase	5 ($n = 5$)	10 ($n = 5$)	20 ($n = 11$)	Total ($n = 21$)
Median age, years (range)	70.0 (28–77)	68.0 (34–78)	68.0 (26–76)	68.0 (26–78)
Male:female	1:4	2:3	3:8	6:15
Underlying anemia, *n* (%)				
MDS	2 (40.0)	3 (60.0)	7 (63.6)	12 (57.1)
AA	3 (60.0)	1 (20.0)	2 (18.2)	6 (28.6)
Other anemias[b]	0	1 (20.0)	2 (18.2)	3 (14.3)
Blood intake during the extension phase, median units/month[c] (range)	4.4 (0–9.6)	4.3 (0–6.1)	3.9 (3.0–13.2)	4.4 (0–15.7)

MDS, myelodysplastic syndromes; *AA*, aplastic anemia

[a] Other anemias: pure red cell aplasia ($n = 3$), myelofibrosis ($n = 1$)

[b] Other anemias: pure red cell aplasia ($n = 2$), myelofibrosis ($n = 1$)

[c] 1 unit = 200 mL

Table 2). As a result of the criteria of dose reduction and interruption shown in Sect. 2.3, dosing was reduced and interrupted in five (23.8%) and eight (38.1%) patients, respectively, because of adverse events (AEs). Seven patients (33.3%) stopped treatment during the extension phase: four (19.0%) because of AEs; two (9.5%) because of improvements in their serum ferritin values; and one (4.8%) because of insufficient nutrition due to family circumstances. In study 0104, five, six, and seven patients were dosed with deferasirox 10, 20, and 40 mg/(kg day), respectively [19].

3.3 Safety and tolerability

Deferasirox was generally well tolerated, and reported AEs were infrequent and mild in severity. No deaths were reported during the study. In the single- and multiple-dose phase, the most common AEs with a reported relationship to deferasirox were diarrhea [7.7%; $n = 2$ each after single and multiple doses of 30 mg/(kg day)], nausea [7.7%; $n = 1$ each after multiple doses at 10 and 30 mg/(kg day)], and non-progressive increases in serum creatinine [7.7%;

Table 2 Duration of treatment, dose adjustments, and discontinuations during the extension phase

	Deferasirox dose [mg/(kg day)]			
	5 ($n = 5$)	10 ($n = 5$)	20 ($n = 11$)	Total ($n = 21$)
Median treatment duration, days (range)	361 (231–365)	365 (197–365)	365 (71–374)	365 (71–374)
Dose adjustments				
Increase, *n* (%)	3 (60.0)	3 (60.0)	1 (9.1)	7 (33.3)
Decrease due to AEs, *n* (%)	0	0	5 (45.5)	5 (23.8)
Interruption due to AEs, *n* (%)	2 (40.0)	2 (40.0)	4 (36.4)	8 (38.1)
Interruption due to symptom improvement, *n* (%)	1 (20.0)	0	2 (18.2)	3 (14.3)
Discontinuations				
Symptom improvement, *n* (%)	1 (20.0)	1 (20.0)	0	2 (9.5)
AEs, *n* (%)	1 (20.0)	1 (20.0)	2 (18.2)	4 (19.0)
Family circumstances[a], *n* (%)	1 (20.0)	0	0	1 (4.8)

AEs, adverse events

[a] Insufficient nutrition

$n = 1$ each after multiple doses at 5 and 30 mg/(kg day)]. One of the 26 patients (3.8%) had two serious AEs, pyrexia and duodenal ulcer, during the multiple-dose phase after doses of 30 mg/(kg day). A relationship with study drug could not be excluded as a cause of this event, although the patient had experienced occasional upper GI symptoms before starting the study.

During the extension phase, the most common AEs with a reported relationship to deferasirox were non-progressive increases in serum creatinine (>33% from baseline value or >ULN at two consecutive visits), increased urine β2-microglobulin, and increased blood alkaline phosphatase (Table 3). Increases in serum creatinine were seen most frequently in the 20 mg/kg dose group, 4–8 weeks after the start of treatment. In patients with increased serum creatinine, a dose reduction or interruption was required most frequently in patients in the higher (20 mg/kg) dose group whose amount of blood transfusion was low [<7 mL/(kg month)].

One of the 21 patients receiving deferasirox 20 mg/(kg day) had a transient increase in liver transaminase levels. Deferasirox treatment was interrupted for 1 week, which led to a reduction in transaminase levels. Deferasirox was restarted at 20 mg/(kg day), and no subsequent increase in transaminases was observed; treatment continued at the same dose.

There were two serious AEs with a suspected relationship to deferasirox administration, both in patients treated at 20 mg/(kg day): one of the 21 patients suffered pharyngeal ulceration and another had interstitial nephritis. Deferasirox therapy was stopped in both cases. The patient with pharyngeal ulceration had a pharyngeal tumorectomy and recovered 7 months after removal from the study, while in the case of interstitial nephritis, the patient's serum creatinine and BUN improved but she was removed from the study 10 weeks after the start of the treatment because her serum creatinine did not return to the initial value. Two other dose discontinuations were due to dementia and progressive multifocal leukoencephalopathy, and these were unrelated to study drug.

3.4 Pharmacokinetic and pharmacodynamic evaluation

3.4.1 Pharmacokinetic evaluation

After single and multiple doses (at steady state), dose-proportional C_{max} and AUC were observed (Table 4; Fig. 2). At steady-state, C_{max} and AUC were approximately 1–2-fold higher than following single-dose administration. The PK parameters (C_{max} and AUC) of deferasirox measured in these Japanese patients were

Table 3 Treatment-related adverse events occurring in ≥2 patients in the extension phase

	Initial deferasirox dose [mg/(kg day)]			
	5 ($n = 5$)	10 ($n = 5$)	20 ($n = 11$)	Total ($n = 21$)
Total adverse drug reactions, *n*	0	1 (20.0)	10 (90.9)	11 (52.4)
Increased serum creatinine[a], *n* (%)	0	0	6 (54.5)	6 (28.6)
Increased urine β2-microglobulin, *n* (%)	0	0	4 (36.4)	4 (19.0)
Increased serum alkaline phosphatase, *n* (%)	0	0	3 (27.3)	3 (14.3)

[a] Non-progressive increase >33% from baseline value or >ULN at two consecutive visits

Table 4 Pharmacokinetic parameters of deferasirox after the single- and multiple-dose phases

Dose (mg/kg)	t_{max} (h)	C_{max} (μmol/L)	AUC_{0-24} (μmol h/L)	$t_{1/2}$ (h)
Day 1 (single dose)				
5 ($n = 6$)	2.0 (0.9–3.0)	20.4 ± 6.1	190 ± 91	8.5 ± 3.4
10 ($n = 7$)	3.0 (1.0–4.0)	53.3 ± 18.7	535 ± 137	17.1 ± 4.7
20 ($n = 6$)	4.0 (1.0–10.0)	112 ± 29	1,270 ± 366	20.5 ± 4.9
30 ($n = 7$)	3.0 (2.0–4.0)	119 ± 40	1,450 ± 423	18.9 ± 9.8[a]
Day 14 (multiple dose)				
5 ($n = 6$)	1.5 (1.0–4.0)	27.4 ± 10.7	345 ± 236	17.5 ± 7.2
10 ($n = 7$)	3.0 (1.1–10.0)	67.3 ± 22.2	848 ± 442	20.5 ± 7.5
20 ($n = 6$)	3.4 (1.0–4.2)	119 ± 14	1,510 ± 193	21.4 ± 7.2
30 ($n = 7$)	3.9 (1.0–10.0)	224 ± 100	3,620 ± 2,760	19.5 ± 4.9

Mean ± SD except for t_{max} [median (min–max)]

[a] $n = 6$

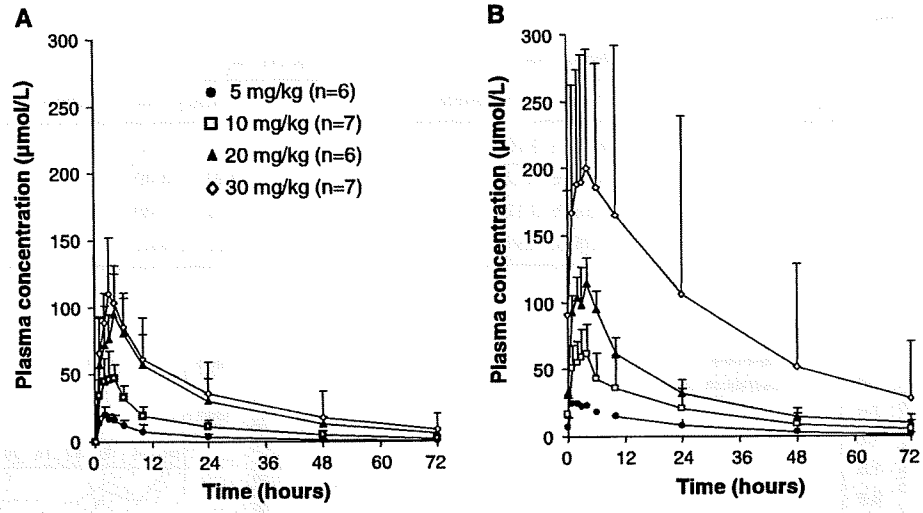

Fig. 2 Plasma concentration–time profiles of deferasirox after **a** single dosing (day 1) and **b** multiple dosing (day 14)

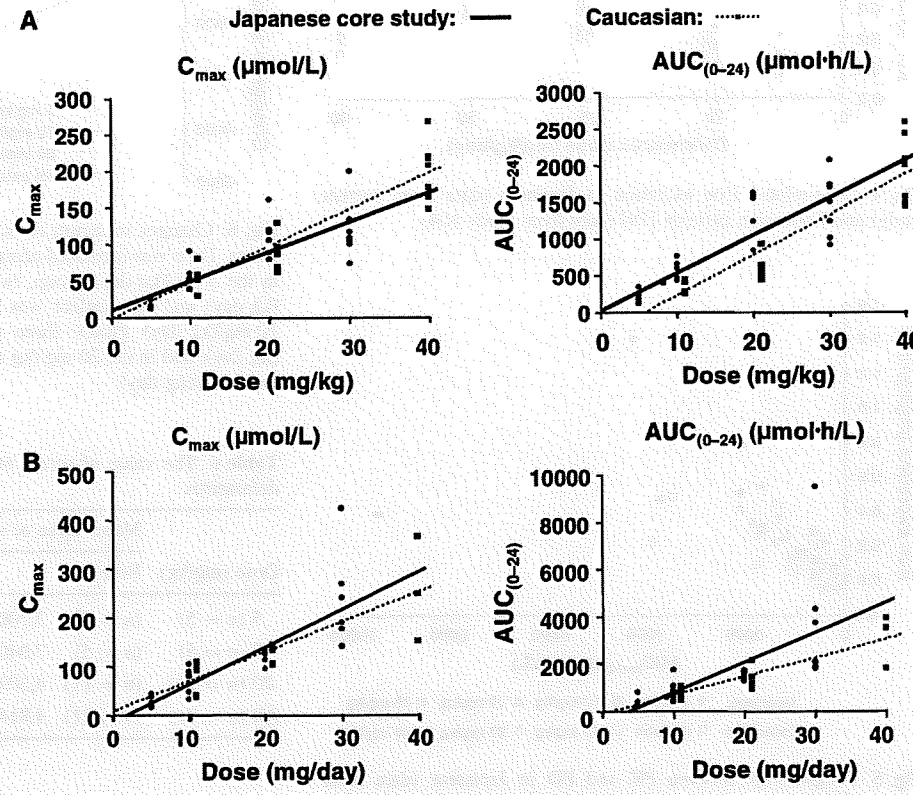

Fig. 3 pharmacokinetics–dose relationship in Japanese (data from current study) and Caucasian patients [19] (data from study 104) after **a** single dosing (day 1) and **b** multiple dosing (day 14)

similar to those measured in Caucasian patients in study 0104 (Fig. 3) [19].

3.4.2 Pharmacodynamic evaluation

One patient in the 5 mg/kg dosing group experienced fecal occult blood and was excluded from the PD data analysis. Dose-dependent iron excretion and a linear relationship between PK (AUC) and PD (iron excretion) were observed (Table 5), with iron excretion being similar to that measured in the Caucasian patients in study 0104 (range 0.12–0.45 mg iron/(kg day); Figs. 4, 5).

3.5 Changes in serum ferritin levels

Changes in levels of serum ferritin were assessed as a marker of iron stores. At the start of the extension phase, median serum ferritin levels were 4,500 μg/L (range

Table 5 Iron excretion

Dose (mg/kg)	Mean iron excretion rate ± SD [mg/(kg day)]		
	Fecal iron excretion	Urinary iron excretion	Total iron excretion
5 ($n = 6$)	0.07 ± 0.10	0.01 ± 0.00	0.07 ± 0.10
10 ($n = 7$)	0.12 ± 0.12	0.01 ± 0.00	0.13 ± 0.12
20 ($n = 6$)	0.33 ± 0.12	0.02 ± 0.00	0.34 ± 0.12
30 ($n = 7$)	0.58 ± 0.39	0.02 ± 0.01	0.61 ± 0.39

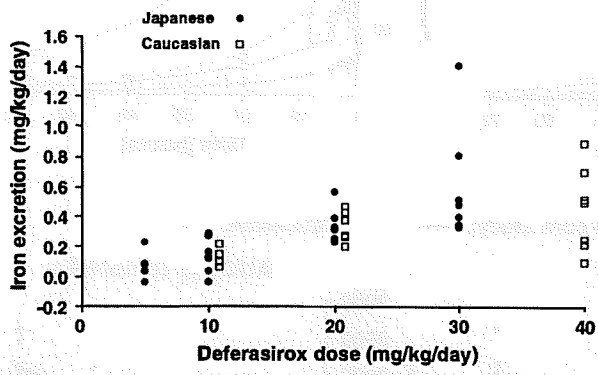

Fig. 4 Dose-related iron excretion in Japanese (data from current study) and Caucasian patients [19] (data from study 104)

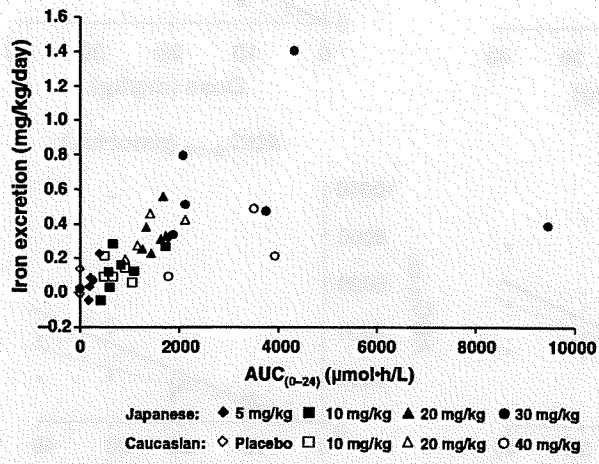

Fig. 5 Relationship between PK and PD in Japanese (data from current study) and Caucasian patients [19] (data from study 104)

1,400–17,000). After 1 year, all patients in the 20 mg/(kg day) group had a decrease in their serum ferritin levels, indicating a negative iron balance, as did four of five patients in the 10 mg/(kg day) group and two of five patients in the 5 mg/(kg day) group. However, these results include dose increases according to the dose adjustment protocol: in the 5 mg/(kg day) group, two patients were increased to 10 mg/(kg day) and one patient was increased

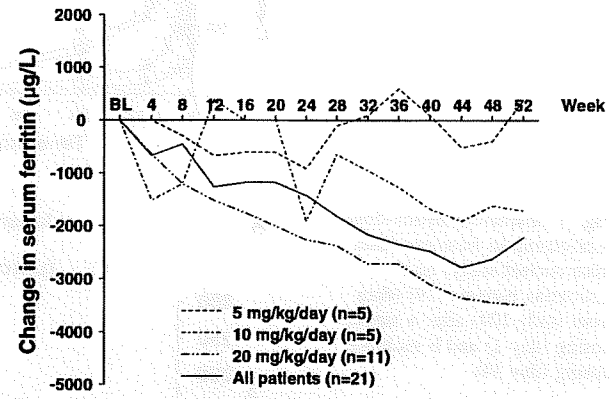

Fig. 6 Changes in serum ferritin following administration of deferasirox. Dose was increased according to the dose adjustment protocol: in the 5 mg/(kg day) group, two patients were increased to 10 mg/(kg day) and one patient was increased to 20 mg/(kg day); in the 10 mg/(kg day) group, three patients were increased to 20 mg/(kg day); and in the 20 mg/(kg day) group, one patient was increased to 30 mg/(kg day)

Table 6 The value of serum ferritin in baseline and after 1 year of deferasirox

Dose (mg/kg)	Mean value of serum ferritin ± SD (μg/L)			
	Baseline		After 1 year (52 weeks)	
5 ($n = 5$)	($n = 5$)	3,700 ± 2,203	($n = 3$)	4,267 ± 1,012
10 ($n = 5$)	($n = 5$)	7,040 ± 5,719	($n = 3$)	4,533 ± 1,747
20 ($n = 11$)	($n = 11$)	4,309 ± 1,865	($n = 8$)	1,243 ± 496
All ($n = 21$)	($n = 21$)	4,814 ± 3,307	($n = 14$)	2,596 ± 1,843

to 20 mg/(kg day); in the 10 mg/(kg day) group, three patients were increased to 20 mg/(kg day); and in the 20 mg/(kg day) group, one patient was increased to 30 mg/(kg day). The median serum ferritin level after 1 year of deferasirox treatment fell by 3,485 μg/L in the 20 mg/(kg day) group and by 1,700 μg/L in the 10 mg/(kg day) group; the median serum ferritin level rose by 400 μg/L in the 5 mg/(kg day) group (Fig. 6). The mean values of serum ferritin at each dose of deferasirox in baseline and after 1 year of deferasirox treatment is shown in Table 6.

4 Discussion

Deferasirox is a once-daily oral iron chelator that allows flexible dosing, adjustable to transfusional iron intake, and therapeutic goal (decrease or maintenance of total body iron). This study assessed the safety, PK, and PD of deferasirox in Japanese patients with chronic anemias and transfusion-dependent iron overload in order to compare with data obtained in Caucasian patients with transfusion-dependent β-thalassemia and secondary iron overload [19].

Deferasirox was generally well tolerated with a manageable safety profile after daily dosing for up to 1 year. The incidence and severity of AEs related to study treatment appeared to be dose dependent, although low patient numbers in each group limit a conclusion. The AE profile in Japanese patients was similar to that seen in previous studies of Caucasian patients with MDS, with no additional safety concerns [15]. Potential AEs in Japanese patients could, therefore, be expected to be anticipated and managed in a similar way to those in non-Japanese patients [21]. Mild increase of serum creatinine to >33% above baseline levels and interstitial nephritis has been observed in the patients treated at 20 mg/kg. After the initial increase, the creatinine levels have remained stable and transient increases in the urinary excretion of β2-microglobulin were observed in some patients. These findings may relate to pre-existing proximal renal tubular damage, which has been attributed to the toxic effects of iron deposits in the kidneys. Investigations are ongoing to explore the effects of deferasirox on the kidney. Meanwhile, serum creatinine should be monitored monthly in all patients.

Exposure to deferasirox was dose dependent with a linear PK/PD relationship, resulting in dose-dependent iron excretion. The PK/PD parameters in the Japanese patients were similar to those seen in the Nisbet-Brown et al. Caucasian β-thalassemia cohort (Study 0104), suggested that deferasirox has a stable and predictable PK/PD, regardless of underlying disease or race. Although efficacy was not evaluated in this study, assessment of serum ferritin levels as an indicator of iron stores indicates that the high iron load of this patient population was reduced after 1 year's deferasirox therapy, and a negative iron balance was achieved in the 20 mg/(kg day) dose group. In a previous study of deferasirox in non-Japanese patients with MDS, and a similar mean iron intake level to the Japanese patients in the current study, doses of 20 and 30 mg/(kg day) were also shown to maintain or reduce iron levels.

In conclusion, this study demonstrates that the PK/PD profile of deferasirox in iron-overloaded Japanese patients with transfusion-dependent anemias is consistent with that previously reported in Caucasian patients [19], with safety and tolerability profiles similar to previous deferasirox studies [21].

References

1. Olivieri N. Thalassaemia: clinical management. Baillieres Clin Haematol. 1998;11:147–62.
2. Jansen AJ, Essink-Bot ML, Beckers EA, Hop WC, Schipperus MR, Van Rhenen DJ. Quality of life measurement in patients with transfusion-dependent myelodysplastic syndromes. Br J Haematol. 2003;121:270–4.
3. Lee MT, Piomelli S, Granger S, et al. Stroke prevention trial in sickle cell anemia (STOP): extended follow-up and final results. Blood. 2006;108:847–52.
4. McLaren GD, Muir WA, Kellermeyer RW. Iron overload disorders: natural history, pathogenesis, diagnosis, and therapy. Crit Rev Clin Lab Sci. 1983;19:205–66.
5. Kushner JP, Porter JP, Olivieri NF. Secondary iron overload. Hematology Am Soc Hematol Educ Program. 2001;47–61.
6. Gabutti V, Piga A. Results of long-term iron-chelating therapy. Acta Haematol. 1996;95:26–36.
7. Olivieri NF, Nathan DG, MacMillan JH, et al. Survival in medically treated patients with homozygous β-thalassemia. N Engl J Med. 1994;331:574–8.
8. Olivieri NF, Brittenham GM. Iron-chelating therapy and the treatment of thalassemia. Blood. 1997;89:739–61.
9. Cortelezzi A, Cattaneo C, Cristiani S, et al. Non-transferrin-bound iron in myelodysplastic syndromes: a marker of ineffective erythropoiesis? Hematol J. 2000;1:153–8.
10. Porter JB, Abeysinghe RD, Marshall L, Hider RC, Singh S. Kinetics of removal and reappearance of non-transferrin-bound plasma iron with deferoxamine therapy. Blood. 1996;88:705–13.
11. Cabantchik ZI, Breuer W, Zanninelli G, Cianciulli P. LPI-labile plasma iron in iron overload. Best Pract Res Clin Haematol. 2005;18:277–87.
12. Takatoku M, Uchiyama T, Okamoto S, et al. Retrospective nationwide survey of Japanese patients with transfusion-dependent MDS and aplastic anemia highlights the negative impact of iron overload on morbidity/mortality. Eur J Haematol. 2007;78:487–94.
13. Gattermann N, Porter JB, Lopes LF, Seymour J. Iron overload in myelodysplastic syndromes. Hematol Oncol Clin North Am. 2005;19 Suppl 1:18–25.
14. Piga A, Galanello R, Forni GL, et al. Randomized phase II trial of deferasirox (Exjade, ICL670), a once-daily, orally-administered iron chelator, in comparison to deferoxamine in thalassemia patients with transfusional iron overload. Haematologica. 2006;91:873–80.
15. Porter J, Galanello R, Saglio G, et al. Relative response of patients with myelodysplastic syndromes and other transfusion-dependent anaemias to deferasirox (ICL670): a 1-yr prospective study. Eur J Haematol. 2008;80:168–76.
16. Cappellini MD, Cohen A, Piga A, et al. A phase 3 study of deferasirox (ICL670), a once-daily oral iron chelator, in patients with β-thalassemia. Blood. 2006;107:3455–62.
17. Vichinsky E, Onyekwere O, Porter J, et al. A randomized comparison of deferasirox versus deferoxamine for the treatment of transfusional iron overload in sickle cell disease. Br J Haematol. 2007;136:501–8.
18. Galanello R, Piga A, Forni GL, et al. Phase II clinical evaluation of deferasirox, a once-daily oral chelating agent, in paediatric patients with β-thalassaemia major. Haematologica. 2006;91:1343–51.